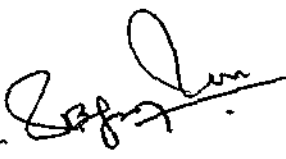
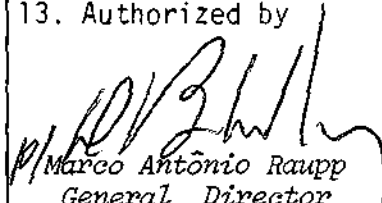


1. Publication Nº <i>INPE-4583-PRE/1317</i>	2. Version	3. Date <i>June 1988</i>	5. Distribution <input type="checkbox"/> Internal <input checked="" type="checkbox"/> External <input type="checkbox"/> Restricted
4. Origin <i>DAS</i>	Program <i>ASTRO</i>		
6. Key words - selected by the author(s) <i>ATMOSPHERIC X AND GAMMA RAYS; PRECIPITATION OF PARTICULES</i>			
7. U.D.C.: <i>52-73</i>			
8. Title <i>X AND GAMMA RAY BACKGROUND OBSERVATIONS IN ANTARCTIC</i>		10. Nº of pages: <i>13</i>	
		11. Last page: <i>12</i>	
		12. Revised by <i>T. Villela</i> <i>Thyrso Villela Neto</i>	
9. Authorship <i>U.B. Jayanthi</i>  Responsible author		13. Authorized by  <i>Marco Antônio Raupp</i> General Director	
14. Abstract/Notes <i>Atmospheric X and gamma rays are products of complex electromagnetic interactions between charged particles and atmospheric constituents. The latitudinal dependence of the cosmic ray secondaries, auroral and South Atlantic Anomaly phenomena produce flux variations especially the later temporal flux variations. We propose to discuss these variations in relevance to balloon flight observations of X and gamma ray atmospheric background at polar latitudes.</i>			
15. Remarks <i>Presented in the "I Seminário sobre Ciências Atmosféricas e Espaciais do Programa Antártico Brasileiro", São José dos Campos (SP).</i>			

X AND GAMMA RAY BACKGROUND OBSERVATIONS IN ANTARCTIC

U.B. Jayanthi

INPE - Instituto de Pesquisas Espaciais

Caixa Postal 515

12201 - São José dos Campos - SP

ABSTRACT

Atmospheric X and gamma rays are products of complex electromagnetic interactions between charged particles and atmospheric constituents. The latitudinal dependence of the cosmic ray secondaries, auroral and South Atlantic Anomaly phenomena produce flux variations, especially the later temporal flux variations. We propose to discuss these variations in relevance to balloon flight observations of X and gamma ray atmospheric background at polar latitudes.

1. INTRODUCTION

X-ray and low energy gamma-ray continua produced in the atmosphere are predominated by the process of bremsstrahlung from electrons. The source of these electrons in general are cosmic rays and in some latitude regions due to precipitation electrons.

Primary cosmic rays initiate cascade process in the atmosphere and produce secondary electrons. The three principal processes are: decay of charged mesons ($\pi^\pm \rightarrow \mu^\pm \rightarrow e^\pm$), the decay of neutral mesons and subsequent pair production ($\pi^0 \rightarrow 2\gamma \rightarrow e^+, e^-$), and knock-on process. Low energy gamma radiation has superposed line at 0.511 keV due to annihilation of e^+ , e^- and capture and inelastic scattering of neutrons by atmospheric nuclei produce lines at 2.31, 4.44 and 6.13 MeV etc.

The X and gamma radiation background variations due to cosmic ray rigidity dependance and precipitation processes are described below.

2. ANTARCTIC REGION

The antarctic region extending between 60° S latitude to South Pole is an excellent place for studies of many geophysical phenomena. With cosmic ray cut-off rigidity reaching much below 3 GV, many cosmic-ray secondary effects can be studied through X and gamma ray background measurements in balloon experiments. The antarctic region is adjacent to South Atlantic Anomaly and incorporates Southern Auroral Zone. In Figure 1, we show the geographical distribution of the 100 KeV electrons at lower altitudes obtained from the data of Seward (1973). The

background measurements with balloon borne experiments can discern the effects due to precipitations of electrons.

a) South Atlantic Anomaly Phenomena

The region of very low surface field in the South Atlantic is expected to be a region of strong interaction between trapped radiation and upper atmosphere. The particle precipitation, greater at the times of intense geomagnetic storms produce bremsstrahlung radiation. Balloon experiments in X-ray and gamma radiation have earlier permitted determination of the electron precipitation in SAA region (Martin et al, 1974, Pinto and Gonzalez, 1985). In Figure 2, at the time of magnetic activity, the gamma-ray count rate (profile a) has a lower decrease between 120 mbrar and 3.5 mbar when compared to charge particle count rate (profile b). The quiet-day radiation obtained (c) in an earlier experiment also supports this excess (Martin et al, 1974).

b) Auroral Zone Phenomena

Electron precipitation in auroral zone is a general feature. The X and gamma radiation fluxes show regular increases ~ 20% over background values. In Figure 3, the results of a balloon flight experiment in northern auroral zone by Anderson (1960) is shown. These increases up to above 340 keV with fine structure of minutes, last typically few hours. The X-ray fluxes in other experiments, during magnetic storms, showed increases by factors 2 to 6 (Winckler et al, 1959, Anderson et al, 1958). Power spectrum analysis of X-ray bursts observed by Winckler (1959) has indicated micropulsations with period $P = 0.8$ sec in coincidence with riometer and magnetic data (Tepley and Wentworth, 1962). These suggest precipitation of

bunched electrons oscillating along geomagnetic field lines.

c) Latitudinal Effect due to Cosmic Rays

The energy of the primary cosmic ray that enter the atmosphere is governed by the earth's dipole magnetic field. While at the equatorial region the energy of the particle that can enter is ≥ 16 GeV, very low energy particles ~ 0.1 GeV reach polar latitudes. Since the flux of the cosmic rays is higher at low energies, interactions in the atmosphere produce higher fluxes of X-ray and gamma-ray continuum at polar latitudes. In addition diurnal and solar modulations of cosmic-ray flux are predominant at low energies and are expected to produce discernable effects in X and gamma radiation background. In Figure 4 we present the variation in X-ray flux and the line flux at 0.51 MeV due to different rigidities conducted by various experimenters. In Figure 4a, the atmospheric X-ray flux (I_{AXR}) increases by factor ~ 7 , for rigidity variation between 16 to 2 GV, where the instrumental effects (I_{CRIB}) are small (Kasturirangan, 1971). The annihilation line flux at 0.511 KeV has 10 factor increase with increase in latitude as shown in Figure 4b (Jayanthi et al, 1982).

3. ZENITH ANGLE VARIATIONS OF FLUX

Direct translation of the cascade and transport of secondary particles to explain the observed photons have been attempted (References: Ling 1975). These calculations are especially not satisfactory to explain the low energy gamma-ray continuum. An inverse of the problem, namely to determine the source function of flux has been attempted from observed data (Vette 1962, Peterson et al 1973 and

Ling 1975). The isotropic source function $S(E,X)$ in a Semi-Empirical Method (SEM) is defined as the production of gamma-rays of energy E , in a unit air mass at a depth X . The production of gamma-rays includes bremsstrahlung of cosmic rays, π^0 decay, nuclear gamma rays, e^- and e^+ annihilation and Compton shifted photons inside the source volume as shown in Figure 5 (Ling, 1975). The SEM does not inquire into the nature of the production processes but attempts to obtain $S(E,X)$, from observations of gamma-ray spectra at different altitudes (above Pfotzer maximum) at any particular latitude, in a self consistent manner. The estimation of source function is useful in predicting the energy and angular dependence of photon fluxes. In Figure 6 (Ling, 1975), the estimate of these dependences at different altitudes, from omnidirectional detector data made at Palestine (Texas), shows the usefulness of the concept of SEM in experiments.

4. BANTAR X-RAY EXPERIMENT

An X-ray detection equipment was flown in a balloon experiment in February 21, 1985 from Comandante Ferraz Base in Antarctic for the determination of source function and any time variation in flux (Jayanthi et al, 1987). The telescope employed a 1.27 cm thick NaI(Tl) crystal with diameter 7.62 cm. Thin Pb shields of ~ 1 mm thick defined the field of view ($\sim 30^\circ$ at 100 keV) for forward X-rays and total obstruction for lateral incident X-rays. The assembly had active anti charged particle shield of NE 104 scintillator. The X-ray detector events not in coincidence with the particle shield were inputted simultaneously to a 32 channel energy analyser in the 28.5 to 185 KeV range and a 64 msec resolution time analyser of total flux.

The payload which attained a ceiling altitude of $\sim 7 \text{ gm cm}^{-2}$, transmitted useful data only in two broad segments of altitude - 985 to 215 mbar and 22.2 to 6.85 mbar, due to telemetry noise problems. The spectra obtained at the ceiling and different altitudes are satisfactory with spectral index $\alpha = 2.0 \pm 0.2$. As the flight terminated prematurely we could not determine any temporal variations. The ceiling data in conjunction with the data from other experiments was utilized to determine the angular variation of X-ray flux.

We have evaluated the ratio R between upward and downward fluxes at different altitudes for our cut-off rigidity ($CR \sim 3.1$). The value of the ratio R , at 7 gm cm^{-2} varies between 2.57 and 1.55, as shown in Figure 7 with an average value of $\sim 2.2 \pm 0.35$ for the 28 to 123 KeV atmospheric X-ray flux. As no data exist for X-rays in literature, this can be compared with R values ~ 2.4 and 4.7 at 300 keV and 1 MeV respectively by Ling (1975) at 7 gm cm^2 and $\sim 3.7, 3.85$ and 5.6 at $2.5, 5.0$ and 10.0 MeV respectively by Hsieh (1978) in low energy gamma region. The up/down flux ratio of $R \sim 2.2$ for the X-rays is consistent with the higher gamma-ray values as the higher absorption mean free path for X-rays produce lower build-up effects in cascade process.

FIGURE CAPTION

Fig. 1: Geographical distribution of the observations of 100 keV electrons at altitudes between 240 and 400 km. South Atlantic Anomaly and Auroral Zone are shown clearly (Seward, 1973).

Fig. 2: Count rate profiles of gamma rays (a) and charged particles (b) of the balloon flight on Oct. 20, 1973. Similar flight as a quiet day (Martin et al, 1974).

Fig. 3: Four channel pulse height analyser data from Scintillation detector flown in balloon experiment in Northern Auroral Zone. Precipitation excess is evident (Anderson, 1960).

Fig. 4: X and gamma ray flux variation with geomagnetic latitude: a) Ratio of Atmospheric X-ray flux (I_{AXR}) to instrumental effects (I_{CRIB}); b) gamma ray line flux at 0.511 MeV (Kasturirangan, 1971; Jayanthi et al, 1982).

Fig. 5: Geometry for calculating the count rate of a detector due to atmospheric gamma rays for an isotropic source function (Ling, 1974).

Fig. 6: Angular distribution of atmospheric gamma ray flux at 3.5 g cm^{-2} . Dashed lines indicate atmospheric flux calculations on the basis of SEM. Solid lines represent inclusion of cosmic gamma rays (Ling, 1974).

Fig. 7: Variation of the computed up/down atmospheric X-ray flux ratio (R) with energy and altitude (Jayanthi et al, 1986).

REFERENCES

- ANDERSON, K.A. *Soft radiation events at high altitude during the magnetic storm of August 29-30, 1957.* Phys. Rev. III: 1397-1405.
- ANDERSON, K.A. *Balloon observations of X-rays in the auroral zone.* J. Geophys. Res., 65:551-564, 1960.
- HSIEH, L.S. *Atmospheric neutron and gamma ray fluxes and energy spectra at balloon altitudes.* Ph. D. Thesis, University of New Hampshire, New Hampshire, 1978.
- JAYANTHI, U.B.; BLANCO, F.G.; AGUIAR, O.D.; JARDIM, J.O.D.; BENSON, J.L.; MARTIN, I.M.; RAO, K.R. *Spectral observations of atmospheric gamma ray background.* Rev. Bras. Fis., 12:431-442, 1982.
- JAYANTHI, U.B.; CORRÊA, R.V.; BLANCO, F.G. *Measurements of Atmospheric X and Gamma Rays - Balloon Experiments at Subantarctic Region.* Rev. Br. Geofis., 4: 149-153, 1986.
- KASTURIRANGAN, K. *Secondary background properties of X-ray astronomical telescopes at balloon altitudes.* J. Geophys. Res., 76: 3527-3533, 1971.
- LING, C.J. *A semi-empirical model for atmospheric gamma rays from 0.3 to 10 MeV at $\lambda = 40^\circ$.* J. Geophys. Res., 80:3241-3252, 1975.
- MARTIN, I.M.; RAI, D.B.; DA COSTA, J.M.; PALMEIRA, R.A.R.; TRIVEDI, N.B. *Enhanced electron precipitation in*

brazilian magnetic anomaly in association with sudden commencement. Nature, 240:84, 1972.

PETERSON, L.; SCHWARTZ, D.A.; LING, J.C. *Spectrum of atmospheric gamma rays to 10 MeV at $\lambda = 40^\circ$.* J. Geophys. Res., 78:7942, 1973.

PINTO JR., O.; GONZALEZ, W.D. *X-ray measurements at the south atlantic magnetic anomaly.* J. Geophys. Res. 91:7072-7078, 1985.

SEWARD, F.D. *The geographical distribution of ~ 100 keV electrons above the earth's atmosphere.* Lawrence Livermore Laboratory, University of California, Livermore (UCRL 51456), 1973.

WINCKLER, J.R.; PETERSON, L.; HOFFMAN, R.; ARNOLDY, R. *Auroral X-rays, cosmic rays and related phenomena during the storm of February 10-11, 1958.* J. Geophys. Res., 64: 597-611, 1959.

TEPLEY, L.R.; WENTWORTH, R.C. *Hydromagnetic emissions, X-ray bursts and electron bunches - experimental results.* J. Geophys. Res., 67: 3317-3333, 1962.

VETTE, J.I. *Low energy gamma rays produced in air and in lead by cosmic rays.* J. Geophys. Res., 67: 1731, 1962.

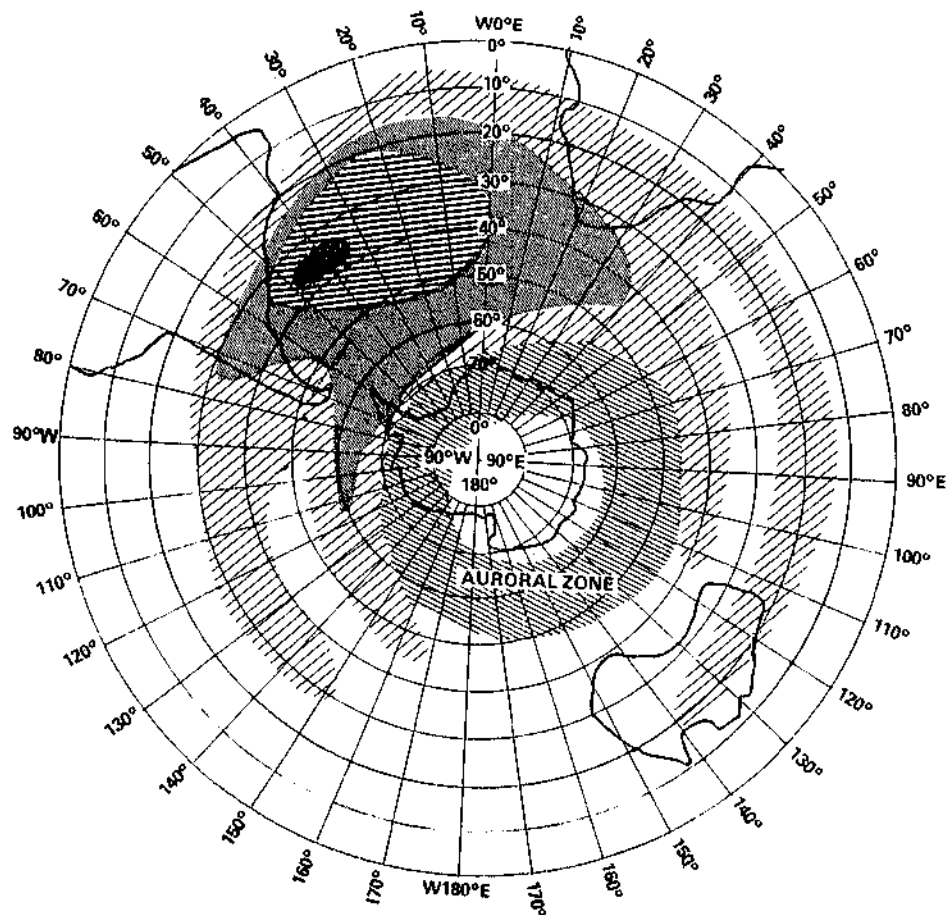


Figure 1

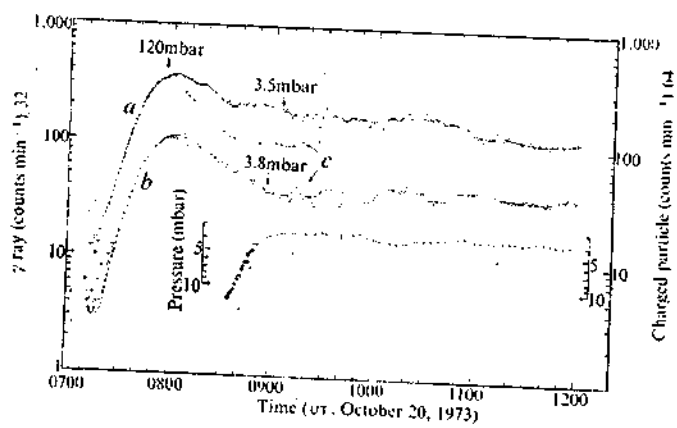


Figure 2

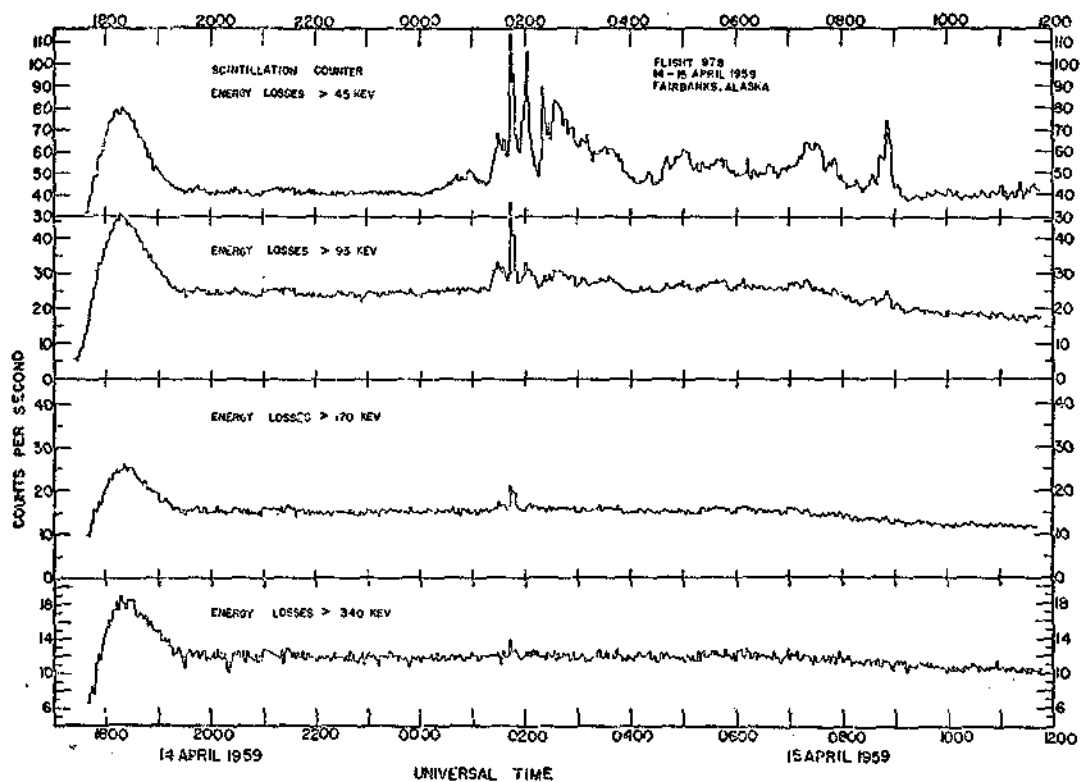


Figure 3

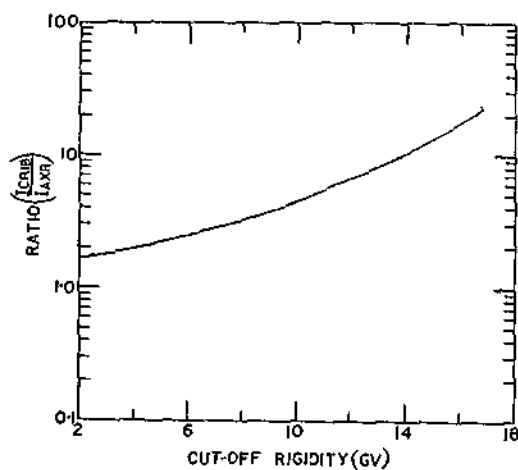


Figure 4a

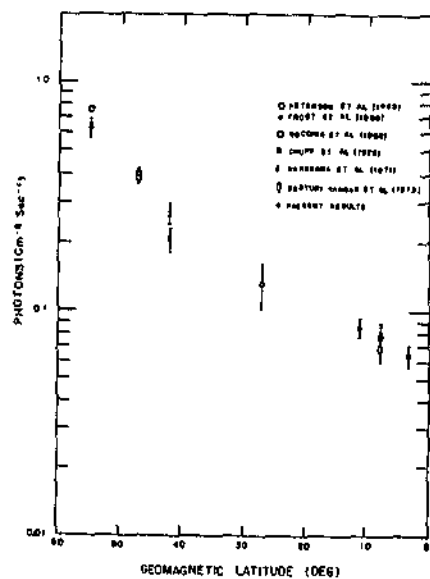


Figure 4b

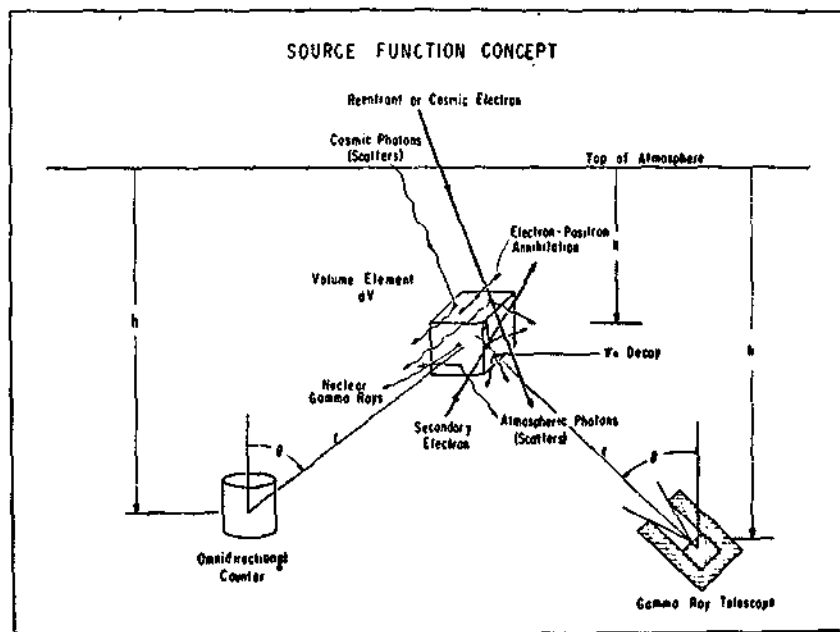


Figure 5

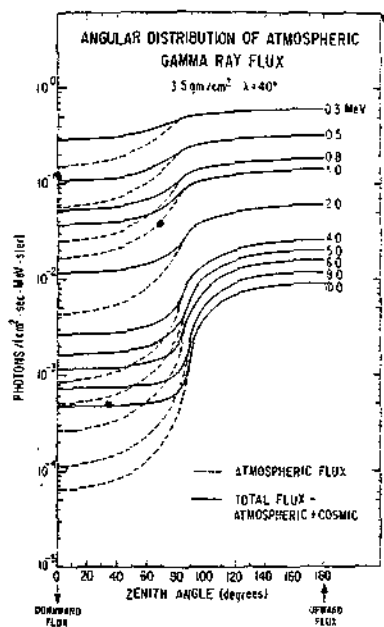


Figure 6

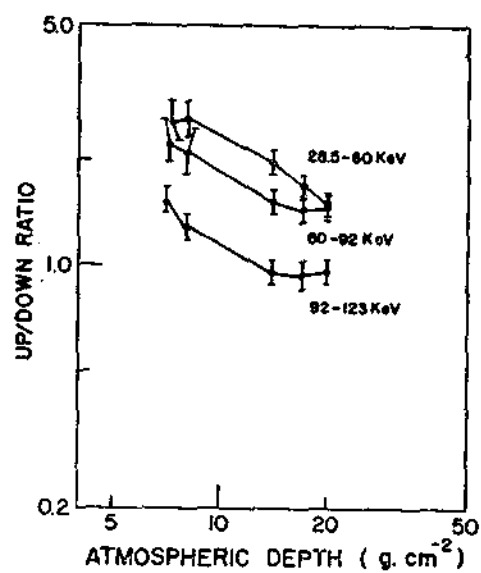


Figure 7